Journal of Science and Technology in Civil Engineering, HUCE, 2023, 17 (3): 1–20

DETERMINATION OF INFLUENCE LINES FOR STRUCTURAL RESPONSES WITH UNCERTAINTIES IN PROPERTIES OF THE STRUCTURE

Thanh Xuan Nguyen[a,*], Anh Tay Nguyen[b]

[a]*Faculty of Building and Industrial Construction, Hanoi University of Civil Engineering, 55 Giai Phong road, Hai Ba Trung district, Hanoi, Vietnam*
[b]*Department of Mechanical Engineering, Northwestern University Evanston, Illinois, USA*

Article history:
Received 08/6/2023, Revised 30/6/2023, Accepted 13/7/2023

Abstract

Classical ways of determination of influence lines for structural responses are often inefficient due to high computational cost, especially if properties of the structure are uncertain. The combination of Muller-Breslau principle and the finite element analysis can resolve this problem. In this study, formulations for new finite elements tailored for use in determination of influence lines for structural responses are proposed. They are then used in the problem of uncertainty propagation to obtain uncertain ordinates of the influence lines. The expressions for the element stiffness matrix and equivalent nodal load vector are derived consistently from the proposed displacement field of the element. The proposed finite elements can be adapted directly in existing finite element packages since they do not need remeshing. Studied examples show the correctness and the efficiency of the proposed method. From the results of uncertainty propagation problem, large uncertainties in the ordinates of influence lines for structural responses due to small uncertainties in structural properties should be aware of.

Keywords: equivalent load vector; finite element method; influence line; Muller-Breslau principle; reciprocal theorem; uncertainty propagation.

https://doi.org/10.31814/stce.huce2023-17(3)-01

1. Introduction

The concept of influence lines and influence surfaces plays a significant role in analyzing structures subjected to moving load conditions. Influence lines or influence surfaces (mentioned from hereafter as influence functions, or IFs) for a response quantity S at a particular point or cross-section of a structure is a plot showing the variation of S with respect to the coordinate(s) of a unit load $P = 1$, with unchanged direction and sense, moving on a lane or a surface of the structure. The IF can be anything that varies as the load moves on the lane across the span or on a part of the structure, such as bending moment or shear force at a given section in the girder or beam, or axial force in a particular truss member. The IF can also be a reaction at a support or a deflection at a given point on the structure. From the help of IFs, the two main tasks in studying structures subjected to moving loads, namely the one for determining the most unfavorable location of the load chain and the one for determining the critical (peak) value of quantity S in consideration due to this (moving) load chain, can be solved more efficiently. Other applications of IFs can be named as damage location and parameter/severity estimation [1].

Since IFs are of immense importance, the certainty of an IF is of great concern. In case there exist uncertainties in properties of the structure, they are propagated to the IF and the immediate question

*Corresponding author. *E-mail address:* thanhnx@huce.edu.vn (Nguyen, T. X.)

is that how certain is the just obtained IF. In addition, related to the issue of uncertainty propagation, to increase the accuracy and the efficiency of the computations, the intermediate computation steps in the structural analysis should be as few as possible, especially for large structures. However, the traditional way to construct an IF, directly based on its definition, does not satisfy this requirement, since the structure is repeatedly analyzed, with one particular onset of structural properties, to find the value of quantity S with each of many different positions of the unit load $P = 1$ applying to the structure on the loading lane or loading surface. With a particular onset of structural properties, it is quite easy to apply this traditional way for the cases dealing with statically determinate frame structures and the response quantity S being a support reaction or one of internal forces. In such a case, the IF is a piece-wise straight curve graph, and indeed, with a particular onset of structural properties, there were already many methods for fast drawing it. With another onset of structural properties, the procedure described above is repeated to find the corresponding IF for S. The traditional way, including the methods for fast drawing an IF for S, is direct and simple. It has, however, limitations and disadvantages when dealing with the case when the quantity S other than a reaction or an internal force, and/or the case where the structure is statically indeterminate. In such often-met situation, it cannot outline the shape of the IF for S before tedious and detailed calculations. Also, since the structure is repeatedly analyzed with various locations of the unit load $P = 1$, the computational cost and time is large, making the traditional way of drawing the IF for S inefficient, even not to mention about the issue of uncertainty propagation.

Practically, many methods proposed to determine IFs do not follow traditional ways but are based on the Muller-Breslau principle which initially dealt with the quantity S of the force type (i.e., it did not cover the case where S is a displacement response of the structure). In [2], Belegundu claimed that this principle is not suitable for finite element implementation. But in 1991, [3] showed the contrary. The algorithm they developed based on Muller-Breslau principle and can be applicable to frames and shells. The procedure falls within the range of standard capabilities offered by most commercial finite element codes. However, this method requires revising the input data, since extra nodes and constraints should be defined to be able to give a relative unit displacement according to the Muller-Breslau principle. In [4], Shen has extended the Muller-Breslau principle to structures consisting of finite elements by introducing a loading vector for average stress at any point on the structure. The method focused on plate structures and is based on the average stress which requires a fine mesh around the point considered for accuracy reason. In [5], Memari and West proposed a remedy for the adjoint method suggested by [2] in case when the response function is in the directions of constrained degrees of freedom of a plate structure. In [6], a direct determination of influence lines and surfaces by FEM was proposed by Orakdogen and Girgin. Although there is no new element introduced, the element loading matrices are defined for static application of classical Muller-Breslau principle to finite element method. The proposed method is quite elegant, but it requires the cross-section should be on the mesh of nodes. In addition, determination of influence lines for a reaction at a support need special treatment involved with two or more elements connected to that support. Recently, in [7], Yang et al. proposed techniques for constructing IFs that based directly on the ordinary differential equation (ODE) of beams to find their deflected shape which represents the associated IF. In [8], the approach offered by Welleman and Eldik is also based on the ODE of beams, but the formulation is shown in matrix notation. In addition, the element corresponding to the case of drawing IF for axial force has not been addressed yet. The approach using FEM was addressed in [9] where the lateral deflection and angular displacements at the point whose S in consideration were determined from static analysis instead of from the rigorous and consistent FEM formula using the assumed

displacement field. The article did not address the case when the direction of the unit load $P = 1$ is not coincident with translational displacement representing the ordinates of the IF. In addition, in the article, the cases where quantity S are translational or rotational displacements were not mentioned. In 2021, Hartmann and Jahn [10] also used FEM for constructing IFs. They offered the local solution as the correction terms. However, the determination of the equivalent nodal load associated with the IFs was not mentioned.

The generalization of the earlier methods, including the case where there exist inclined elements on the lane and/or the case where the unit moving load is not perpendicular to the element axis, has not been found yet. Also, in case the quantity S is an internal force, for the convenient use of existing finite element mesh without large modification, there is a need to establish finite elements whose displacement field is not continuous, to be used in constructing IFs for S inside those elements. To some extents, this can be considered as the development of the work of [9], stated in FEM language, with the formulation consistently inspired by the principle of stationary potential energy and strictly established from the assumed displacement fields. By this way, no correction term is needed in the results of displacements of the element containing the quantity S. Also, by this way, it can make ease to extend to the problem of drawing influence surfaces in plate bending structures. From literature review, there is no research on the construction of influence lines or influence surfaces in the presence of uncertainties in the structural properties. In other words, the uncertainty propagation from the structural properties to IFs for response quantity S has not been addressed so far in any earlier study. Therefore, this article will solve the problem of uncertainty propagation from structural properties to influence lines with the proposed finite elements. The paper is organized as follows. In Section 2, techniques for constructing commonly met influence lines are represented and finite elements formulations are developed. In Section 3, the problem of uncertainty propagation is summarized and a tool for the implementation of uncertainty propagation, written in Julia language, is introduced. Examples in Section 4 illustrate the use of the proposed finite elements. Section 5 will finalize the article with conclusions and further studies suggested.

2. Finite elements tailored for constructing influence lines

2.1. Reciprocal theorems applied in constructing influence lines

As mentioned earlier, although the ordinates of an IF for any response quantity S may be obtained by placing a unit load successively at each load point on the structure, this procedure becomes a long and tedious process. The Muller-Breslau principle can be used to greatly reduce computational efforts in determining IFs. Essentially, this principle is rooted from reciprocal theorems in structural mechanics which were mentioned earlier by Betti in 1872 [11] and then was explored in brief details in [12]. Particularly, two of these theorems used here in determining IFs are Maxwell reciprocal theorem [13] and Gvozdev reciprocal theorem [14] whose statements are given below

$$\delta_{ij} = \delta_{ji}, \quad \breve{r}_{ij} = -\breve{\delta}_{ji} \tag{1}$$

where δ_{ij} is the displacement along the ith degree of freedom (DOF) of the structure, due to unit load applied along the jth DOF of the same structure; $\breve{r}_{ij}$ is the reaction associated with the ith restrained DOF of the structure, due to unit load applied along the jth DOF of the same structure; and $\breve{\delta}_{ji}$ is the displacement along the jth DOF of the structure, due to unit displacement imposed at the ith restrained DOF of the same structure. More specifically, they are used suitably case-by-case depending on the particular quantity S as follows.

In case the quantity S for which the influence line is to be drawn is a displacement at a cross-section, from the Maxwell reciprocal theorem, the influence line can be found by solving for the

displacement field of the dual problem in which the same structure is subjected to a fixed unit load associated with the quantity S. For example, if we need to draw the influence line for a lateral deflection at a cross-section k, instead of successively applying an unit moving load along the lane and finding this lateral deflection, we can just find the deformed shape of the same structure when it is subjected to a fixed lateral load of unit magnitude applied at cross-section k. Similarly, if we need to draw the influence line for a rotational displacement at k, we can just find the deformed shape of the same structure when it is subjected to a fixed moment of unit magnitude applied at cross-section k. By doing in such way, the amount of computational effort is reduced greatly and under the view's point of finite element analysis, there is no additional complexity introduced. Particularly, we can use the same stiffness matrix, the same procedure to generate the equivalent load vector, and the same representation of displacement field through the same shape functions for the interpolation of any desired displacement. Also, note that the equivalent load vector is remarkably simple with only few non-zero components associated with the finite element containing the displacement quantity S in consideration.

In case the quantity S for which the influence line is to be drawn is a reaction at a support, from the Gvozdev reciprocal theorem, the influence line can be found by solving for the displacement field of the dual problem in which the same structure is subjected to an imposed translational/rotational displacement of unit magnitude associated with the quantity S, but in reverse direction. For example, if we need to draw the influence line for a force reaction at a roller support, instead of successively applying an unit moving load along the lane and finding this force reaction, we can just find the deformed shape of the same structure when it is subjected to an imposed translational displacement of unit magnitude at the roller support, and in reverse direction. Similarly, if we need to draw the influence line for a moment reaction at a fixed support, we can just find the deformed shape of the same structure when it is subjected to an imposed rotational displacement of unit magnitude associated with the fixed support and in reverse direction. By doing in such way, the amount of computational effort is also reduced greatly. Also, under the view's point of finite element analysis, there is no additional complexity introduced since the imposed displacement of unit magnitude at a support can be simply defined in the model as a boundary condition.

The situation becomes more complicated when the quantity S for which the influence line being drawn is an internal force at a cross-section k. Of course, we also want a solution better than applying successively a unit moving load along the lane and finding this internal force. In this situation, a better way to construct the influence line is as follows. First, a proper component of internal connection at k should be released. Now, according to the Gvozdev reciprocal theorem, a pair of imposed displacements whose magnitude difference is equal to unit is applied to the structure. The resulting deformed shape of the structure is coincident with the influence line in consideration. For the least modification of the existing FEM packages, this research proposes a new treatment to deal firstly with the discontinuity in the element introduced by releasing a component of internal connection and then with the pair of imposed displacement occurred inside the element. The proposed method is general for other types of structures but is presented here for the frame structures in two dimensions only.

2.2. Development of finite elements tailored for IFs

a. Displacement field representation

M-type finite element

For a finite element associated with the problem of drawing influence line for bending moment M_k, we consider the element shown in Fig. 1 where a hinge is introduced at the cross-section k instead of a weld connection there. The hinge separates the whole element into two segments. There are two

inner compatibility conditions for this whole element. The first one is that the lateral displacements v of both segments at the two sides of the hinge should be equal

$$v\left(a^{-}\right) = v\left(a^{+}\right) \tag{2}$$

where a is the distance from the left end of the element to the hinge in its local coordinate system, $v\left(a^{-}\right)$ is the lateral displacement of the cross-section just next to the left of the hinge, and $v\left(a^{+}\right)$ is the corresponding one just next to the right of the hinge. The second inner compatibility condition requires that the rotational displacement just next to the left of the hinge and the one just next to the right of the hinge differ by one unit in their values.

$$\varphi\left(a^{+}\right) - \varphi\left(a^{-}\right) = 1 \tag{3}$$

where $\varphi\left(a^{+}\right)$ is the rotational displacement of the cross-section just next to the right of the hinge, and $\varphi\left(a^{-}\right)$ is the rotational displacement of the cross-section just next to the left of the hinge. These rotations can be found from the first derivative of the lateral displacement $v\left(x\right)$ with respect to the coordinate x.

In addition, the continuity conditions for the internal forces of the two cross-sections just next to the two sides of the hinges

$$M\left(a^{-}\right) = M\left(a^{+}\right), \quad V\left(a^{-}\right) = V\left(a^{+}\right) \tag{4}$$

will, for the linear problems, lead to

$$v''\left(a^{-}\right) = v''\left(a^{+}\right), \quad v'''\left(a^{-}\right) = v'''\left(a^{+}\right) \tag{5}$$

Thus, for this M-type finite element, the displacement field, satisfying the conditions mentioned above, can be assumed as follows

$$u\left(x\right) = \alpha_0 + \alpha_1 x, \quad \left(0 \le x \le \ell\right) \tag{6}$$

$$v\left(x\right) = \begin{cases} \beta_0 + \beta_1 x + \beta_2 x^2 + \beta_3 x^3, & \left(0 \le x \le a^{-}\right) \\ \left(\beta_0 - a\right) + \left(\beta_1 + 1\right) x + \beta_2 x^2 + \beta_3 x^3, & \left(a^{+} \le x \le \ell\right) \end{cases} \tag{7}$$

where ℓ is the length of the element, and coefficients α_0, α_1, β_0, β_1, β_2, and β_3 are to be found from the nodal displacements at the two ends of the element, denoted as from q_1 to q_6 as shown in Fig. 1.

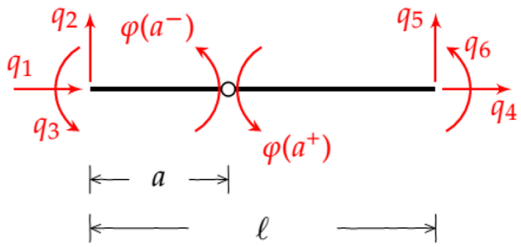

(a) Positive sign convention for nodal DOFs and the discontinuity in rotational displacement at $x = a$

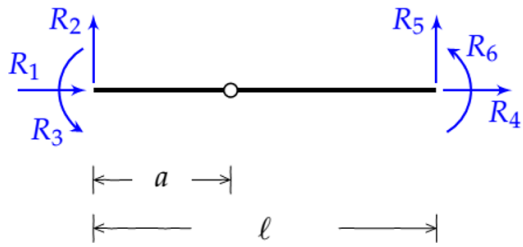

(b) The corresponding equivalent nodal load $\mathbf{R}_M$

Figure 1. M-type finite element

By applying these boundary conditions

$$u\left(0\right) = q_1, \quad u\left(\ell\right) = q_4 \tag{8}$$

$$v\left(0\right) = q_2, \quad \varphi\left(0\right) = v'\left(0\right) = q_3, \quad v\left(\ell\right) = q_5, \quad \varphi\left(\ell\right) = v'\left(\ell\right) = q_6 \tag{9}$$

all coefficients $\alpha_0, \alpha_1, \beta_0, \beta_1, \beta_2$, and β_3 are found and $\mathbf{u} = [u(x)\ v(x)]^T$ can be now rewritten as

$$\mathbf{u} = \begin{bmatrix} N_1(x) & 0 & 0 & N_4(x) & 0 & 0 \\ 0 & N_2(x) & N_3(x) & 0 & N_5(x) & N_6(x) \end{bmatrix} \mathbf{q} + \begin{bmatrix} 0 \\ C_M(x) \end{bmatrix} = \mathbf{N}\mathbf{q} + \mathbf{C}_M \tag{10}$$

where $\mathbf{q} = \begin{bmatrix} q_1 & q_2 & \dots & q_6 \end{bmatrix}^T$ and

$$\mathbf{N} = \begin{bmatrix} N_1(x) & 0 & 0 & N_4(x) & 0 & 0 \\ 0 & N_2(x) & N_3(x) & 0 & N_5(x) & N_6(x) \end{bmatrix} \tag{11}$$

with shape functions from $N_1(x)$ to $N_6(x)$ being the same as in traditional finite 2D beam elements

$$\begin{aligned} N_1(x) &= 1 - \frac{x}{\ell}, \quad N_2(x) = 1 - \frac{3x^2}{\ell^2} + \frac{2x^3}{\ell^3}, \quad N_3(x) = x - \frac{2x^2}{\ell} + \frac{x^3}{\ell^2}, \\ N_4(x) &= \frac{x}{\ell}, \quad N_5(x) = \frac{3x^2}{\ell^2} - \frac{2x^3}{\ell^3}, \quad N_6(x) = -\frac{x^2}{\ell} + \frac{x^3}{\ell^2} \end{aligned} \tag{12}$$

The vector $\mathbf{C}_M = \begin{bmatrix} 0 & C_M(x) \end{bmatrix}^T$ with $C_M(x)$ given in (13) is the moment-related add-on term that is complementary to the formulation $\mathbf{u} = \mathbf{N}\mathbf{q}$ of the traditional finite 2D beam element.

$$C_M(x) = \begin{cases} \dfrac{(3a - 2\ell)x^2}{\ell^2} + \dfrac{(\ell - 2a)x^3}{\ell^3}, & (0 \le x \le a^-) \\ -a + x + \dfrac{(3a - 2\ell)x^2}{\ell^2} + \dfrac{(\ell - 2a)x^3}{\ell^3}, & (a^+ \le x \le \ell) \end{cases} \tag{13}$$

V-type finite element

For a finite element associated with the problem of drawing influence line for shear force V_k, regarding the normal convention of positive sign of shears, the two inner compatibility conditions are as follows

$$v(a^+) - v(a^-) = -1, \quad \varphi(a^+) = \varphi(a^-) \tag{14}$$

The continuity conditions for the internal forces

$$M(a^-) = M(a^+), \quad V(a^-) = V(a^+) \tag{15}$$

will, for the linear problems, also lead to

$$v''(a^-) = v''(a^+), \quad v'''(a^-) = v'''(a^+) \tag{16}$$

Thus, for this V-type finite element, the displacement field, satisfying the conditions mentioned above, can be assumed as follows

$$u(x) = \alpha_0 + \alpha_1 x, \quad (0 \le x \le \ell) \tag{17}$$

$$v(x) = \begin{cases} \beta_0 + \beta_1 x + \beta_2 x^2 + \beta_3 x^3, & (0 \le x \le a^-) \\ (\beta_0 - 1) + \beta_1 x + \beta_2 x^2 + \beta_3 x^3, & (a^+ \le x \le \ell) \end{cases} \tag{18}$$

Denote q_1 to q_6 as the element nodal displacements shown in Fig. 2.

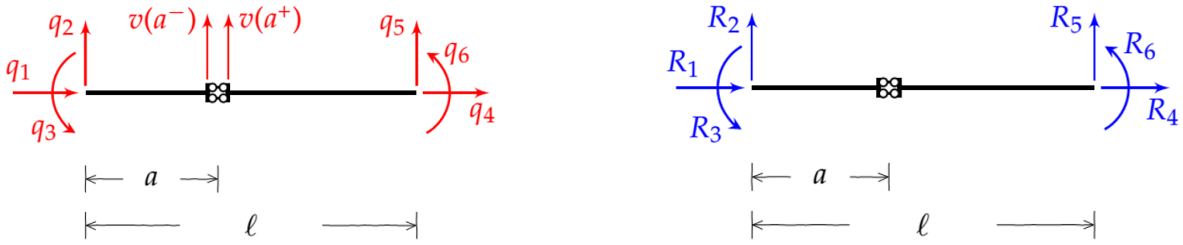

(a) Positive sign convention for nodal DOFs and the discontinuity in lateral displacement at $x = a$

(b) The corresponding equivalent nodal load $\mathbf{R}_V$

Figure 2. V-type finite element

After applying the boundary conditions at the two ends of the element, we will have

$$\mathbf{u} = \mathbf{N}\mathbf{q} + \mathbf{C}_V \tag{19}$$

where the matrix $\mathbf{N}$ of shape functions is the same as before and

$$\mathbf{C}_V = \begin{bmatrix} 0 \\ C_V(x) \end{bmatrix}, \quad C_V(x) = \begin{cases} N_5(x), & (0 \le x \le a^-) \\ -N_2(x), & (a^+ \le x \le \ell) \end{cases} \tag{20}$$

T-type finite element

For a finite element associated with the problem of drawing influence line for axial force T_k, the inner compatibility condition is

$$u(a^+) - u(a^-) = 1 \tag{21}$$

The continuity conditions for the internal axial force

$$T(a^-) = T(a^+) \tag{22}$$

will, for the linear problems, also lead to

$$u'(a^-) = u'(a^+) \tag{23}$$

Thus, for this T-type finite element, the displacement field, satisfying the conditions mentioned above, can be assumed as follows

$$u(x) = \begin{cases} \alpha_0 + \alpha_1 x, & (0 \le x \le a^-) \\ (\alpha_0 + 1) + \alpha_1 x, & (a^+ \le x \le \ell) \end{cases} \tag{24}$$

$$v(x) = \beta_0 + \beta_1 x + \beta_2 x^2 + \beta_3 x^3, \quad (0 \le x \le \ell) \tag{25}$$

Denote q_1 to q_6 as the element nodal displacements shown in Fig. 3.

After applying the boundary conditions at the two ends of the element, we will have

$$\mathbf{u} = \mathbf{N}\mathbf{q} + \mathbf{C}_T \tag{26}$$

where the matrix $\mathbf{N}$ of shape functions is the same as before and

$$\mathbf{C}_T = \begin{bmatrix} C_T(x) \\ 0 \end{bmatrix}, \quad C_T(x) = \begin{cases} -N_4(x), & (0 \le x \le a^-) \\ N_1(x), & (a^+ \le x \le \ell) \end{cases} \tag{27}$$

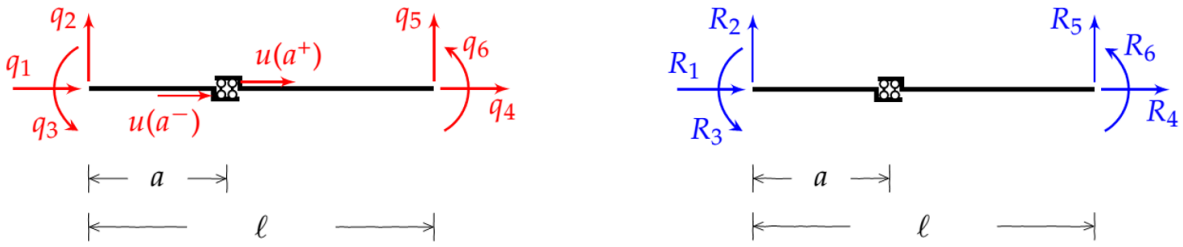

(a) Positive sign convention for nodal DOFs and the discontinuity in axial displacement at $x = a$

(b) The corresponding equivalent nodal load $\mathbf{R}_T$

Figure 3. T-type finite element

b. The strain and stress fields

The strain vector at an infinitesimally small fiber of the cross-section, located at the distance y from the neutral axis, is obtained as

$$\boldsymbol{\varepsilon} = \varepsilon = \boldsymbol{\nabla}\mathbf{u} = \boldsymbol{\nabla}\left(\mathbf{N}\mathbf{q} + \mathbf{C}\right) = \mathbf{B}\mathbf{q} + \boldsymbol{\nabla}\mathbf{C} \tag{28}$$

where $\mathbf{B} = \boldsymbol{\nabla}\mathbf{N}$ and $\boldsymbol{\nabla}$ is the partial differential operator which, for the case of frame elements in two-dimension problem, is

$$\boldsymbol{\nabla} = \begin{bmatrix} \dfrac{\partial}{\partial x} & -y\dfrac{\partial^2}{\partial x^2} \end{bmatrix} \tag{29}$$

The vector $\mathbf{C}$ is null for all finite elements except the only one element which contains the internal force quantity S for which the influence line is to be drawn.

Assuming that the material is in the linear range, the corresponding stress vector is obtained as

$$\boldsymbol{\sigma} = \sigma = \mathbf{D}\boldsymbol{\varepsilon} = \mathbf{D}\left(\mathbf{B}\mathbf{q} + \boldsymbol{\nabla}\mathbf{C}\right) \tag{30}$$

where the elastic matrix $\mathbf{D}$ is, in the case of frame elements in two dimensions, equal to the Youngs' modulus of elasticity E.

c. Element stiffness matrix and equivalent load vector

The total potential energy $\Pi_p = \dfrac{1}{2}\displaystyle\int_\Omega \boldsymbol{\sigma}^T\boldsymbol{\varepsilon}\mathrm{d}\Omega$ of the element is thus

$$\Pi_p = \frac{1}{2}\mathbf{q}^T\left(\int_\Omega \mathbf{B}^T\mathbf{D}\mathbf{B}d\Omega\right)\mathbf{q} + \mathbf{q}^T\left(\int_\Omega \mathbf{B}^T\mathbf{D}\left(\boldsymbol{\nabla}\mathbf{C}\right)d\Omega\right) + g\left(a, \ell, EI, EA\right) \tag{31}$$

where $g\left(\cdot\right)$ is a function free of the nodal displacement $\mathbf{q}$.

From the principle of stationary potential energy

$$\frac{\mathrm{d}\Pi_p}{\mathrm{d}\mathbf{q}} = 0 \Leftrightarrow \mathbf{K}\mathbf{q} = \mathbf{R} \tag{32}$$

where $\mathbf{K}$, for all considered types of elements above, can be shown to be the same as the usual stiffness matrix.

$$\mathbf{K} = \begin{bmatrix} EA/\ell & 0 & 0 & -EA/\ell & 0 & 0 \\ & 12EI/\ell^3 & 6EI/\ell^2 & 0 & -12EI/\ell^3 & 6EI/\ell^2 \\ & & 4EI/\ell & 0 & -6EI/\ell^2 & 2EI/\ell \\ & & & EA/\ell & 0 & 0 \\ & & & & 12EI/\ell^3 & -6EI/\ell^2 \\ \text{symm.} & & & & & 4EI/\ell \end{bmatrix} \tag{33}$$

where EA is the axial stiffness of the cross-section, and EI is the bending stiffness of the cross-section, and $\mathbf{R}$ is the equivalent load vector.

$$\mathbf{R} = -\int_{\Omega} \mathbf{B}^T \mathbf{D} \left(\nabla \mathbf{C}\right) d\Omega \tag{34}$$

This equivalent load vector is concretized as follows. For the finite element containing the bending moment for which the influence line is to be drawn, vector $\mathbf{R}$ is obtained as below

$$\mathbf{R} = \mathbf{R}_M = \begin{bmatrix} 0 \\ 6EI\left(2a-\ell\right)/\ell^3 \\ 2EI\left(3a-2\ell\right)/\ell^2 \\ 0 \\ 6EI\left(\ell-2a\right)/\ell^3 \\ 2EI\left(3a-\ell\right)/\ell^2 \end{bmatrix} \tag{35}$$

Similarly, for the finite element containing the shear force or the axial force, for which the influence line is to be drawn, vector $\mathbf{R}$ is obtained as below, respectively.

$$\mathbf{R} = \mathbf{R}_V = \begin{bmatrix} 0 \\ 12EI/\ell^3 \\ 6EI/\ell^2 \\ 0 \\ -12EI/\ell^3 \\ 6EI/\ell^2 \end{bmatrix}, \quad \mathbf{R} = \mathbf{R}_T = \begin{bmatrix} -EA/\ell \\ 0 \\ 0 \\ EA/\ell \\ 0 \\ 0 \end{bmatrix} \tag{36}$$

For any other structural elements not containing the quantity S for which the influence line is to be drawn, the vector $\mathbf{R}$ is just equal to zero vector.

Note that if the quantity S is a displacement at a cross-section, vector $\mathbf{R}$ is just simply the usual equivalent load vector induced by applying a (fixed) unit load, associated with the displacement S, to the finite element accordingly. There is no need to use any of the new finite elements in the model in this case. It is also worthy to note that if the quantity S is a reaction in a support, before applying the boundary conditions, the $\mathbf{R}$ is initially just a zero vector, since we impose a unit displacement to the support and thus there is no external load at all. This imposed unit displacement is then treated as a boundary condition of the model as in a conventional finite element analysis procedure. With this treatment, now non-zero vector $\mathbf{R}^*$, after the boundary condition is applied, will be obtained accordingly.

d. Global FEM equations and the displacement field $\mathbf{u}$ revisited

After establishing the stiffness matrix $\mathbf{K}$ and the equivalent load vector $\mathbf{R}$ for all finite elements of the structure, the assembly procedure is implemented as traditionally to have the following global equation

$$\mathbf{K}^*\mathbf{q}^* = \mathbf{R}^* \tag{37}$$

where $\mathbf{K}^*$ is the global stiffness matrix of the structure, $\mathbf{q}^*$ is the nodal displacement vector in the global coordinates, and $\mathbf{R}^*$ is the global equivalent load vector.

Solving Eq. (37) will yield,

$$\mathbf{q}^* = \left(\mathbf{K}^*\right)^{-1} \mathbf{R}^* \tag{38}$$

From vector $\mathbf{q}^*$ obtained above for the system level and in global coordinates, one can derive the vector of nodal displacement $\mathbf{q}$ at the element level and in its local coordinates. Now, for elements containing the quantity S, Eqs. (10), (19), or (26) are used to obtain the displacement field $\mathbf{u}$. For elements not containing the quantity S, the displacement field $\mathbf{u}$ is obtained from vector of nodal displacement $\mathbf{q}$ using conventional procedure as usual. The next step is to calculate any desired displacement associated with the influence line in consideration from vector $\mathbf{u}$ showing the displacement field in the element. In other words, vector $\mathbf{u}$ is needed to project onto the direction of the unit load $P = 1$ for the desired deformed shape of the structure which is corresponding to the ordinates of IFs.

Note that in the above procedure, for a given onset of structural properties, the analysis of structure is implemented just once to have all information of the influence line for the quantity S in consideration.

3. Uncertainty propagation and the tool

3.1. Brief theory of uncertainty propagation

Uncertainty always exists in any models, predictions, and measurements of the system properties. Uncertainty in various inputs can all affect the outputs of the system. When the variables are the values of experimental measurements, they have uncertainties due to measurement limitations (e.g., instrument precision) which propagate due to the combination of variables in the response function. In this article, we consider the type of uncertainty that comes from measurements themselves of system properties. A structural property or parameter such as length of span, cross-section area, and area moment of inertia, Youngs' modulus, ... might be associated with uncertainty if it is, e.g., measured, and subject to measurement error, or otherwise estimated from data. One of the ways to express an uncertain measurement is to use the interval quantities, such as $[a; b]$ where a is the lower bound of the quantity and b is its upper bound. With this way of notation, one can conduct interval finite element analysis to have the structural responses [15]. However, for the convenience of this research, according to [16], an uncertain measurement z can be expressed in two parts: the nominal value $\bar{z}$ and the uncertainty. In this article, it is expressed as $z = \bar{z} \pm \sigma_z$ where the uncertainty is quantified in terms of the standard deviation σ_z. If the uncertainties are correlated, then their covariance matrix must be considered.

Propagation of uncertainty calculates the effects of the uncertainty in structure's properties on the structural responses. This information is critical when quantifying confidence in a particular response. With uncertainty propagation, one can determine whether structural responses will meet requirements given the anticipated variation in structural properties. Then the probabilities of outcomes can be estimated, and the required tolerances can be determined effectively, thus, to predict more chance of failures before they happen.

There are several methods for uncertainty propagation available in literature, among which the sampling-based approximation techniques seem still in widespread practice nowadays, especially for highly nonlinear functions. When function $\mathbf{f}$ is a set of non-linear combination of the uncertain variables z_i, a nonlinear uncertainty propagation could be performed to compute intervals which contain all consistent values of $\mathbf{f}$. In a probabilistic approach, the function $\mathbf{f}$ must usually be linearised by approximation to a first-order Taylor series expansion, though in several cases, exact formulae can be derived that do not depend on the expansion as is the case for the exact variance of products [17]. The Taylor expansion would be:

$$f_k \approx f_k^0 + \sum_{i=1}^{n} \frac{\partial f_k}{\partial z_i} z_i, \quad k = 1, 2, \ldots, n \tag{39}$$

where $\partial f_k/\partial z_i$ denotes the partial derivative of component f_k with respect to the ith variable, evaluated at the nominal value $\bar{z}_i$. Or in matrix notation,

$$\mathbf{f} \approx \mathbf{f}^0 + \mathbf{J}\mathbf{z} \tag{40}$$

where $\mathbf{f}^0$ is the vector composed of all $f_k^0, (k = 1, 2, \ldots, n)$ and $\mathbf{J}$ is the Jacobian matrix. Since $\mathbf{f}^0$ is a constant, it does not contribute to the error on $\mathbf{f}$. Therefore, the propagation of uncertainty follows, in matrix notation, as

$$\mathbf{\Sigma}^{\mathbf{f}} = \mathbf{J}\mathbf{\Sigma}^{\mathbf{z}}\mathbf{J}^T \tag{41}$$

where $\mathbf{\Sigma}^{\mathbf{z}}$ and $\mathbf{\Sigma}^{\mathbf{f}}$ are the variance-covariance matrix of the uncertain measurements $\mathbf{z}$ and of the function $\mathbf{f}$, respectively. Note this is equivalent to the matrix expression for the linear case where the component f_k of $\mathbf{f}$ is a linear combination of n variables $z_1, z_2, \ldots, z_n$. If $z_1, z_2, \ldots, z_n$ are only functional correlated or if their correlations are negligible, then the variance-covariance matrix $\mathbf{\Sigma}^{\mathbf{z}}$ becomes variance matrix with diagonal terms only.

3.2. The tool: MonteCarloMeasurements.jl package in Julia language

While performing computations with deterministic values is straightforward, doing the same from associated probability distributions is, outside a few exceptional cases, highly nontrivial. There raises the need of a tool for dealing with the problem of uncertainty propagation. Although there are already many tools available for this problem, such as *UncertaintyWrapper* and *soerp* packages written in Python or *metRology* package written in R language, the package MonteCarloMeasurement.jl [18] is selected here as the tool of preference. It is because that this tool has performance advantages of the multiple-dispatch paradigm of Julia in providing numerical types that behave like regular numbers, but internally represent and propagate sample-based representations of probability distributions. By this, it can significantly mitigate the computational cost of Monte-Carlo evaluations of a program.

The package uses a core type, called Particles, to represent probability distributions, where the name "Particles" comes from the particle-filtering literature. The type Particles represents the distribution using a vector of unweighted particles and can thus represent arbitrary distributions and handle nonlinear uncertainty propagation well. It is worthy to note that when the quantity S is a nonlinear function of uncertain variables, and/or the uncertain variables do not follow the normal distribution, and/or they are statistically correlated, the complete treatment and full assessment of propagation of these uncertainties to S cannot easily be done with other packages. The package also supports arbitrary correlations (and arbitrary dependencies such as conservation laws etc.) between variables. The type Particles also behave like a distribution, so after a calculation, an approximation to the complete distribution of the output is captured and represented by the output particles whose mean, std etc. can be extracted. Particles can also be assigned to a specific distribution, e.g., normal or Gamma distribution. We can also know other attributes of particles like maximum/minimum, quantile as well [18]. For the sampling, the package performs systematic sampling by making use of quantile function (inverse of cumulative distribution function) to distribute samples in a way that minimizes the discrepancy while exactly obeying the target distribution. Therefore, this tool will be used in the next section to investigate the propagation of uncertainties in structure's properties to the influence lines for structural responses.

4. Examples

Although all calculation steps in the following examples can be done numerically, for the illustration purpose, they are done here symbolically up to the penultimate step, before applying calculations

for uncertainty propagation. Considering the deterministic case, the first example is very simple that can be readily verified, and it just aims to show the correctness of the results when the proposed finite elements are used. Meanwhile, the second example determines the influence lines for structural response quantities with the presence of uncertainties in the structural properties.

4.1. Example 1

Consider a simply supported beam, inclined by an angle α. The request is to draw the influence lines for the bending moment, shear force, and axial force at the cross-section k in the two cases below: (a) the roller support is vertical (Fig. 4a1); and (b) the roller support is perpendicular to the beam axis (Fig. 4a2).

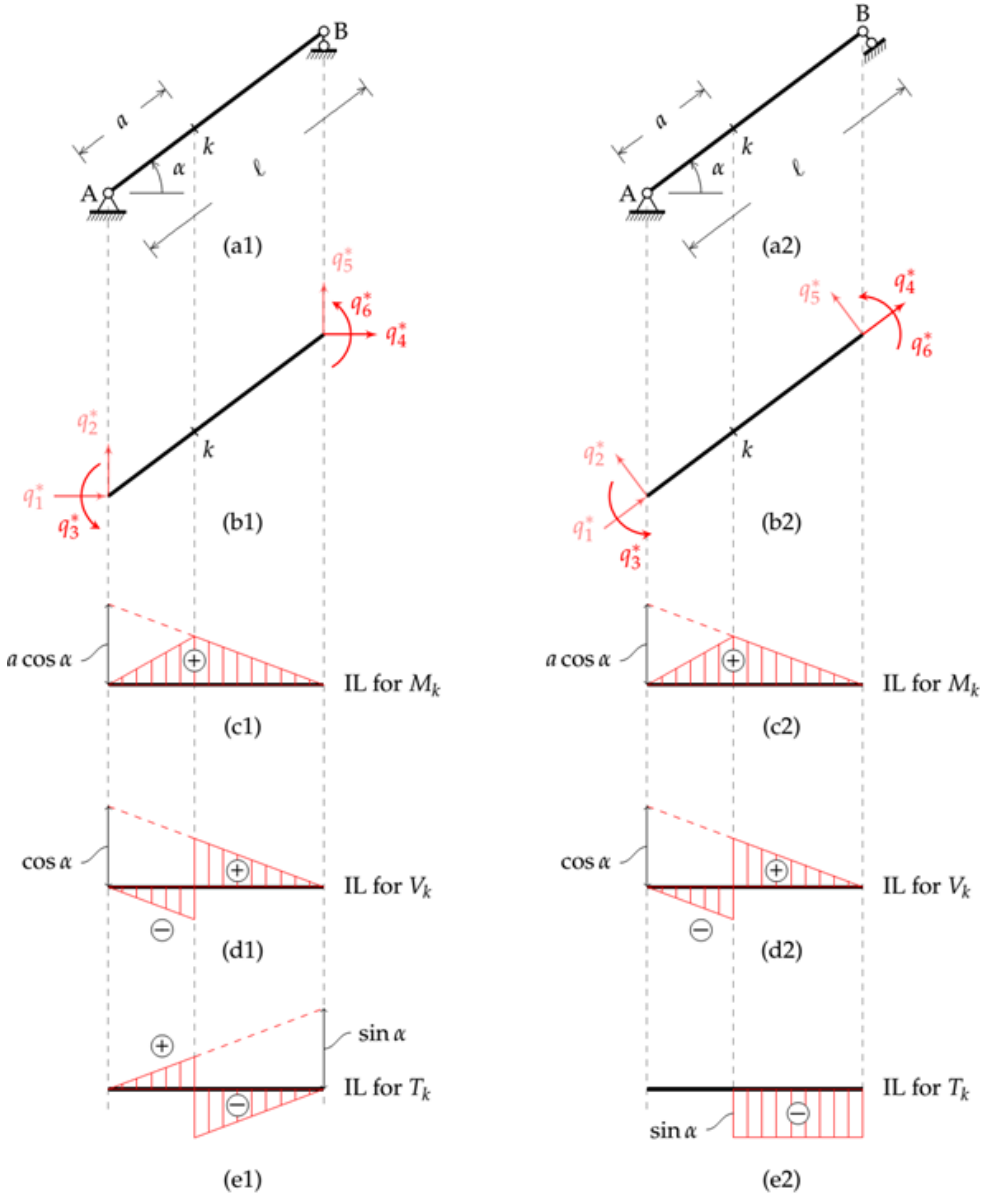

Figure 4. Simply supported beams with a vertical link support (left); and an inclined link support (right)

a. When the roller support is vertical

Denote $c = \cos\alpha$ and $s = \sin\alpha$, the global stiffness matrix after implementing the boundary conditions is the same for three problems of drawing influence lines for M_k, V_k, and T_k as below

$$\mathbf{K}^* = \begin{bmatrix} 4EI/\ell & s\cdot 6EI/\ell^2 & 2EI/\ell \\ & c^2\cdot EA/\ell + s^2\cdot 12EI/\ell^3 & s\cdot 6EI/\ell^2 \\ \text{symm.} & & 4EI/\ell \end{bmatrix} \tag{42}$$

This stiffness matrix is associated with three degrees of freedom q_3^*, q_4^*, and q_6^* shown in Fig. 4a. The equivalent load vectors after implementing the boundary conditions are different for each problem as follows

$$\mathbf{R}_M^* = \begin{bmatrix} 2EI\,(3a-2\ell)/\ell^2 \\ s\cdot 6EI\,(2a-\ell)/\ell^3 \\ 2EI\,(3a-\ell)/\ell^2 \end{bmatrix}, \quad \mathbf{R}_V^* = \begin{bmatrix} 6EI/\ell^2 \\ s\cdot 12EI/\ell^3 \\ 6EI/\ell^2 \end{bmatrix}, \quad \mathbf{R}_T^* = \begin{bmatrix} 0 \\ c\cdot EA/\ell \\ 0 \end{bmatrix} \tag{43}$$

where the indices M, V, and T show the problem of drawing the influence line for M_k, for V_k, and for T_k, respectively.

Solving Eq. (37) for $\mathbf{q}^*$, we have

$$\mathbf{q}_M^* = \begin{bmatrix} (a-\ell)/\ell \\ 0 \\ a/\ell \end{bmatrix}, \quad \mathbf{q}_V^* = \begin{bmatrix} 1/\ell \\ 0 \\ 1/\ell \end{bmatrix}, \quad \mathbf{q}_T^* = \begin{bmatrix} -(s/c)/\ell \\ 1/c \\ -(s/c)/\ell \end{bmatrix} \tag{44}$$

Combining with the zero nodal displacements at boundaries and transforming into the local coordinate will yield,

$$\mathbf{q}_M = \begin{bmatrix} 0 \\ 0 \\ (a-\ell)/\ell \\ 0 \\ 0 \\ a/\ell \end{bmatrix}, \quad \mathbf{q}_V = \begin{bmatrix} 0 \\ 0 \\ 1/\ell \\ 0 \\ 0 \\ 1/\ell \end{bmatrix}, \quad \mathbf{q}_T = \begin{bmatrix} 0 \\ 0 \\ -(s/c)/\ell \\ 1 \\ -s/c \\ -(s/c)/\ell \end{bmatrix} \tag{45}$$

Then, the displacement fields are obtained as following Eqs. (10), (19), and (26)

$$\mathbf{u}_M = \mathbf{N}\mathbf{q}_M + \mathbf{C}_M = \begin{bmatrix} 0 \\ v_M \end{bmatrix}, \quad v_M = \begin{cases} (a-\ell)\,x/\ell; & (0 \le x \le a^-) \\ a\,(x-\ell)/\ell; & (a^+ \le x \le \ell) \end{cases} \tag{46}$$

$$\mathbf{u}_V = \mathbf{N}\mathbf{q}_V + \mathbf{C}_V = \begin{bmatrix} 0 \\ v_V \end{bmatrix}, \quad v_V = \begin{cases} x/\ell; & (0 \le x \le a^-) \\ -1 + x/\ell; & (a^+ \le x \le \ell) \end{cases} \tag{47}$$

$$\mathbf{u}_T = \mathbf{N}\mathbf{q}_T + \mathbf{C}_T = \begin{bmatrix} u_T \\ -(s/c)\,x/\ell \end{bmatrix}, \quad u_T = \begin{cases} 0; & (0 \le x \le a^-) \\ 1; & (a^+ \le x \le \ell) \end{cases} \tag{48}$$

The last step is to transform the displacement field $\mathbf{u}$ in the local coordinates into the normally used coordinates where the downward vertical component displacement (since, by convention, the unit load $P = 1$ is downward) is corresponding to the ordinate of the influence lines. The results are shown in subfigures from Fig. 4c1 to Fig. 4e1.

b. When the roller support is perpendicular to the beam axis

In this case, the global stiffness matrix, preferably represented in local coordinates of the beam, after implementing the boundary conditions is the same for three problems of drawing influence lines for M_k, V_k, and T_k as below

$$\mathbf{K}^* = \begin{bmatrix} 4EI/L & 0 & 2EI/L \\ & EA/L & 0 \\ \text{symm.} & & 4EI/L \end{bmatrix} \tag{49}$$

This stiffness matrix is associated with three degrees of freedom q_3^*, q_4^*, and q_6^* shown in Fig. 4b. Note that the global coordinate system is chosen to be coincident with the local coordinate system. The equivalent load vectors, also in local coordinates of the beam, after implementing the boundary conditions, are different for each problem as follows

$$\mathbf{R}_M^* = \begin{bmatrix} 2EI\left(3a-2\ell\right)/\ell^2 \\ 0 \\ 2EI\left(3a-\ell\right)/\ell^2 \end{bmatrix}, \quad \mathbf{R}_V^* = \begin{bmatrix} 6EI/\ell^2 \\ 0 \\ 6EI/\ell^2 \end{bmatrix}, \quad \mathbf{R}_T^* = \begin{bmatrix} 0 \\ EA/\ell \\ 0 \end{bmatrix} \tag{50}$$

Solving Eq. (37) for $\mathbf{q}^*$, we have

$$\mathbf{q}_M^* = \begin{bmatrix} \left(a-\ell\right)/\ell \\ 0 \\ a/\ell \end{bmatrix}, \quad \mathbf{q}_V^* = \begin{bmatrix} 1/\ell \\ 0 \\ 1/\ell \end{bmatrix}, \quad \mathbf{q}_T^* = \begin{bmatrix} 0 \\ 1 \\ 0 \end{bmatrix} \tag{51}$$

Note that these nodal displacement vectors are already in the local coordinates. Combining with the zero nodal displacements at boundaries and then using Eqs. (10), (19), and (26), we have

$$\mathbf{u}_M = \mathbf{N}\mathbf{q}_M + \mathbf{C}_M = \begin{bmatrix} 0 \\ v_M \end{bmatrix}, \quad v_M = \begin{cases} \left(a-\ell\right)x/\ell, & \left(0 \le x \le a^-\right) \\ a\left(x-\ell\right)/\ell, & \left(a^+ \le x \le \ell\right) \end{cases} \tag{52}$$

$$\mathbf{u}_V = \mathbf{N}\mathbf{q}_V + \mathbf{C}_V = \begin{bmatrix} 0 \\ v_V \end{bmatrix}, \quad v_V = \begin{cases} x/\ell, & \left(0 \le x \le a^-\right) \\ -1 + x/\ell, & \left(a^+ \le x \le \ell\right) \end{cases} \tag{53}$$

$$\mathbf{u}_T = \mathbf{N}\mathbf{q}_T + \mathbf{C}_T = \begin{bmatrix} u_T \\ 0 \end{bmatrix}, \quad u_T = \begin{cases} 0, & \left(0 \le x \le a^-\right) \\ 1, & \left(a^+ \le x \le \ell\right) \end{cases} \tag{54}$$

The last step is to transform the displacement field $\mathbf{u}$ in the local coordinates into the normally used coordinates where the vertical component displacement is corresponding to the ordinate of the influence lines. The results are shown in subfigures from Fig. 4c2 to Fig. 4e2.

It is worthy to note that, if the beam were not straight, it could be splitted into straight finite elements, and the same results as above can be obtained with no additional complexity.

4.2. Example 2

Consider a statically indeterminate multi-span beam as shown in Fig. 5. The request is to draw the influence lines for: (a) vertical deflection y_k; (b) rotational displacement φ_k; (c) force reaction at the roller support B; (d) moment reaction at the fixed end A; (e) bending moment M_k; (f) shear force V_k; and (g) axial force T_k. The structural properties are given as uncertain values below.

$$\begin{gathered} E_1 = 2.3\text{E}7 \pm 1.1\text{E}6, \quad E_2 = 2.5\text{E}7 \pm 1.3\text{E}6, \quad b_1 = 0.3 \pm 0.02, \\ h_1 = 0.5 \pm 0.04, \quad b_2 = 0.3 \pm 0.02, \quad h_2 = 0.4 \pm 0.03 \end{gathered} \tag{55}$$

where E_1 and E_2 are the Youngs' modulus of material of the first and of the second beam, respectively. The cross-sections of the ith beam are assumed to be rectangular of the width b_i and of the height h_i. They are even assumed to be correlated with each other by the following correlation matrix.

$$\mathbf{\Sigma}_1 = \begin{bmatrix} 0.02^2 & 0.0006 \\ 0.0006 & 0.04^2 \end{bmatrix}, \quad \mathbf{\Sigma}_2 = \begin{bmatrix} 0.02^2 & 0.0005 \\ 0.0005 & 0.03^2 \end{bmatrix} \tag{56}$$

The distance a is selected to be one meter to the right of the support B. The units of quantities here are consistent with kN for forces and m for distance. Note that the span lengths L_1 and L_2, in general, can also be uncertain, but for the shake of easily plotting the results, deterministic values of $\ell_1 = 4$ m and $\ell_2 = 3$ m are used here. Also note that there is correlation between the height and the width of the cross-section, resulting in the existence of correlation between area and the area moment of inertia of the cross-section. The software package MonteCarloMeasurements.jl could deal well with this nonlinear uncertainty propagation problem, involving correlations between variables.

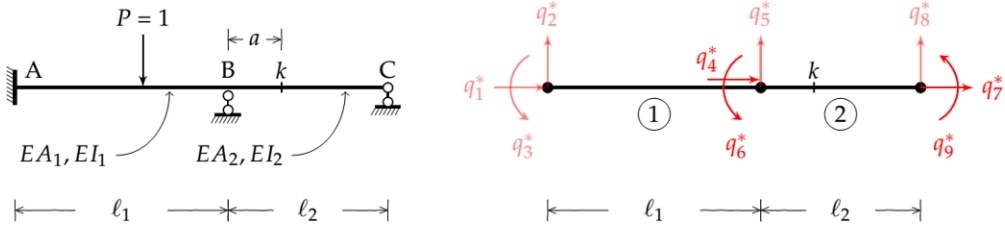

Figure 5. A statically indeterminate structure (left); and its finite element model where the active DOFs are shown in red color, and the inactive DOFs are shown in red color with opacity (right)

In all cases, after applying boundary conditions, the global stiffness matrix associated with the nodal displacement vector $\mathbf{q}^*$ composing the four active DOFs (q_4, q_6, q_7, q_9) is as follows

$$\mathbf{K}^* = \begin{bmatrix} E_1A_1/\ell_1 + E_2A_2/\ell_2 & 0 & -E_2A_2/\ell_2 & 0 \\ & 4\left(E_1I_1/\ell_1 + E_2I_2/\ell_2\right) & 0 & 2E_2I_2/\ell_2 \\ & & E_2A_2/\ell_2 & 0 \\ \text{symm.} & & & 4E_2I_2/\ell_2 \end{bmatrix} \tag{57}$$

Denote the equivalent load vectors after implementing the boundary conditions for problems (a) to (g) as $\mathbf{R}^{a*}, \mathbf{R}^{b*}, \ldots, \mathbf{R}^{g*}$, respectively. For the questions from (a) to (g), from the usual procedure with conventional finite elements and with new finite elements, we have

$$\begin{aligned}
\mathbf{R}^{\mathrm{a}*} &= \begin{bmatrix} 0 & a\left(\ell_2 - a\right)^2/\ell_2^2 & 0 & a^2\left(a - \ell_2\right)/\ell_2^2 \end{bmatrix}^T, \\
\mathbf{R}^{\mathrm{b}*} &= \begin{bmatrix} 0 & \left(\ell_2 - a\right)\left(\ell_2 - 3a\right)/\ell_2^2 & 0 & a\left(3a - 2\ell_2\right)/\ell_2^2 \end{bmatrix}^T, \\
\mathbf{R}^{\mathrm{c}*} &= \begin{bmatrix} 0 & 6\left(E_2I_2/\ell_2^2 - E_1I_1/\ell_1^2\right) & 0 & 6E_2I_2/\ell_2^2 \end{bmatrix}^T, \\
\mathbf{R}^{\mathrm{d}*} &= \begin{bmatrix} 0 & -2E_1I_1/\ell_1 & 0 & 0 \end{bmatrix}^T, \\
\mathbf{R}^{\mathrm{e}*} &= \begin{bmatrix} 0 & 2E_2I_2\left(3a - 2\ell_2\right)/\ell_2^2 & 0 & 2E_2I_2\left(3a - \ell_2\right)/\ell_2^2 \end{bmatrix}^T, \\
\mathbf{R}^{\mathrm{f}*} &= \begin{bmatrix} 0 & 6E_2I_2/\ell_2^2 & 0 & 6E_2I_2/\ell_2^2 \end{bmatrix}^T, \\
\mathbf{R}^{\mathrm{g}*} &= \begin{bmatrix} -E_2A_2/\ell_2 & 0 & E_2A_2/\ell_2 & 0 \end{bmatrix}^T
\end{aligned} \tag{58}$$

Solving Eq. (33) for $\mathbf{q}^{\mathrm{m}*} = \begin{bmatrix} q_4^{\mathrm{m}} & q_6^{\mathrm{m}} & q_7^{\mathrm{m}} & q_9^{\mathrm{m}} \end{bmatrix}^T$ where the index "m" is taken as "a", "b", ..., or "g" will yield,

$$
\begin{aligned}
\mathbf{q}^{\mathrm{a}*} &= \begin{bmatrix} 0 & \dfrac{\ell_1 a\left(2\ell_2^2 - 3\ell_2 a + a^2\right)}{2\ell_2\left(4E_1I_1\ell_2 + 3E_2I_2\ell_1\right)} & 0 & \dfrac{a\left(a-\ell_2\right)\left(2E_1I_1\ell_2 a + E_2I_2\ell_1\left(a+\ell_2\right)\right)}{2E_2I_2\ell_2\left(4E_1I_1\ell_2 + 3E_2I_2\ell_1\right)} \end{bmatrix}^T, \\
\mathbf{q}^{\mathrm{b}*} &= \begin{bmatrix} 0 & \dfrac{\ell_1\left(2\ell_2^2 - 6\ell_2 a + 3a^2\right)}{2\ell_2\left(4E_1I_1\ell_2 + 3E_2I_2\ell_1\right)} & 0 & \dfrac{2E_1I_1\ell_2 a\left(3a-2\ell_2\right) + E_2I_2\ell_1\left(3a^2 - \ell_1\ell_2\right)}{2E_2I_2\ell_2\left(4E_1I_1\ell_2 + 3E_2I_2\ell_1\right)} \end{bmatrix}^T, \\
\mathbf{q}^{\mathrm{c}*} &= \begin{bmatrix} 0 & \dfrac{3\left(E_2I_2\ell_1^2 - 2E_1I_1\ell_2^2\right)}{\ell_1\ell_2\left(4E_1I_1\ell_2 + 3E_2I_2\ell_1\right)} & 0 & \dfrac{3\left(3E_2I_2\ell_1^2 + E_1I_1\ell_2\left(\ell_2 + 2\ell_1\right)\right)}{\ell_1\ell_2\left(4E_1I_1\ell_2 + 3E_2I_2\ell_1\right)} \end{bmatrix}^T, \\
q_5^{\mathrm{c}*} &= -1, \\
\mathbf{q}^{\mathrm{d}*} &= \begin{bmatrix} 0 & \dfrac{-2E_1I_1\ell_2}{4E_1I_1\ell_2 + 3E_2I_2\ell_1} & 0 & \dfrac{E_1I_1\ell_2}{4E_1I_1\ell_2 + 3E_2I_2\ell_1} \end{bmatrix}^T, q_3^{\mathrm{d}*} = -1, \\
\mathbf{q}^{\mathrm{e}*} &= \begin{bmatrix} 0 & \dfrac{3E_2I_2\ell_1\left(a-\ell_2\right)}{\ell_2\left(4E_1I_1\ell_2 + 3E_2I_2\ell_1\right)} & 0 & \dfrac{2E_1I_1\ell_2\left(3a-\ell_2\right) + 3E_2I_2\ell_1 a}{\ell_2\left(4E_1I_1\ell_2 + 3E_2I_2\ell_1\right)} \end{bmatrix}^T, \\
\mathbf{q}^{\mathrm{f}*} &= \begin{bmatrix} 0 & \dfrac{3E_2I_2\ell_1}{\ell_2\left(4E_1I_1\ell_2 + 3E_2I_2\ell_1\right)} & 0 & \dfrac{3\left(2E_1I_1\ell_2 + E_2I_2\ell_1\right)}{\ell_2\left(4E_1I_1\ell_2 + 3E_2I_2\ell_1\right)} \end{bmatrix}^T, \\
\mathbf{q}^{\mathrm{g}*} &= \begin{bmatrix} 0 & 0 & 1 & 0 \end{bmatrix}^T
\end{aligned}
\tag{59}
$$

Note that, for question (c), there is also the imposed displacement $q_5^{\mathrm{c}*} = -1$ besides the obtained $\mathbf{q}^{\mathrm{c}*}$. Similarly, for question (d), there is also the imposed displacement $q_3^{\mathrm{d}*} = -1$ besides the obtained $\mathbf{q}^{\mathrm{d}*}$.

The component $v(x)$ in displacement field in the element 1 and 2 in their local coordinates is corresponding to the ordinate of influence line when the unit load $P = 1$ moving on these elements, respectively. From $\mathbf{q}^*$ obtained above, for each question from (a) to (g), we have the following results

$$
\begin{aligned}
\mathbf{u}^{\mathrm{a,b}} &= \begin{bmatrix} 0 \\ v^{\mathrm{a,b}}(x) \end{bmatrix}, \quad v^{\mathrm{a,b}}(x) = \begin{cases} N_6(x)\, q_6^{\mathrm{a,b}}, & \text{when } P = 1 \text{ on element 1} \\ N_3(x)\, q_6^{\mathrm{a,b}} + N_6(x)\, q_9^{\mathrm{a,b}}, & \text{when } P = 1 \text{ on element 2} \end{cases}, \\
\mathbf{u}^{\mathrm{c}} &= \begin{bmatrix} 0 \\ v^{\mathrm{c}}(x) \end{bmatrix}, \quad v^{\mathrm{c}}(x) = \begin{cases} -N_5(x) + N_6(x)\, q_6^{\mathrm{c}}, & \text{when } P = 1 \text{ on element 1} \\ -N_2(x) + N_3(x)\, q_6^{\mathrm{c}} + N_6(x)\, q_9^{\mathrm{c}}, & \text{when } P = 1 \text{ on element 2} \end{cases}, \\
\mathbf{u}^{\mathrm{d}} &= \begin{bmatrix} 0 \\ v^{\mathrm{d}}(x) \end{bmatrix}, \quad v^{\mathrm{d}}(x) = \begin{cases} -N_3(x) + N_6(x)\, q_6^{\mathrm{d}}, & \text{when } P = 1 \text{ on element 1} \\ N_3(x)\, q_6^{\mathrm{d}} + N_6(x)\, q_9^{\mathrm{d}}, & \text{when } P = 1 \text{ on element 2} \end{cases}, \\
\mathbf{u}^{\mathrm{e,f}} &= \begin{bmatrix} 0 \\ v^{\mathrm{e,f}}(x) \end{bmatrix}, \quad v^{\mathrm{e,f}}(x) = \begin{cases} N_6(x)\, q_6^{\mathrm{e,f}}, & \text{when } P = 1 \text{ on element 1} \\ N_3(x)\, q_6^{\mathrm{e,f}} + N_6(x)\, q_9^{\mathrm{e,f}} + C(x), & \text{when } P = 1 \text{ on element 2} \end{cases}, \\
\mathbf{u}^{\mathrm{g}} &= \begin{bmatrix} 0 \\ v^{\mathrm{g}}(x) \end{bmatrix}, \quad v^{\mathrm{g}}(x) = 0 \quad \text{when } P = 1 \text{ on both elements 1 and 2}
\end{aligned}
\tag{60}
$$

where $C = C_M$ for question (e) and $C = C_V$ for question (f). Note that in this example, the quantity ℓ appeared in $C_M(x)$, $C_V(x)$ and $C_T(x)$ should be substituted by ℓ_2. Note also that the unit load $P = 1$ is downward, and the obtained displacement field should be projected on this downward vertical direction.

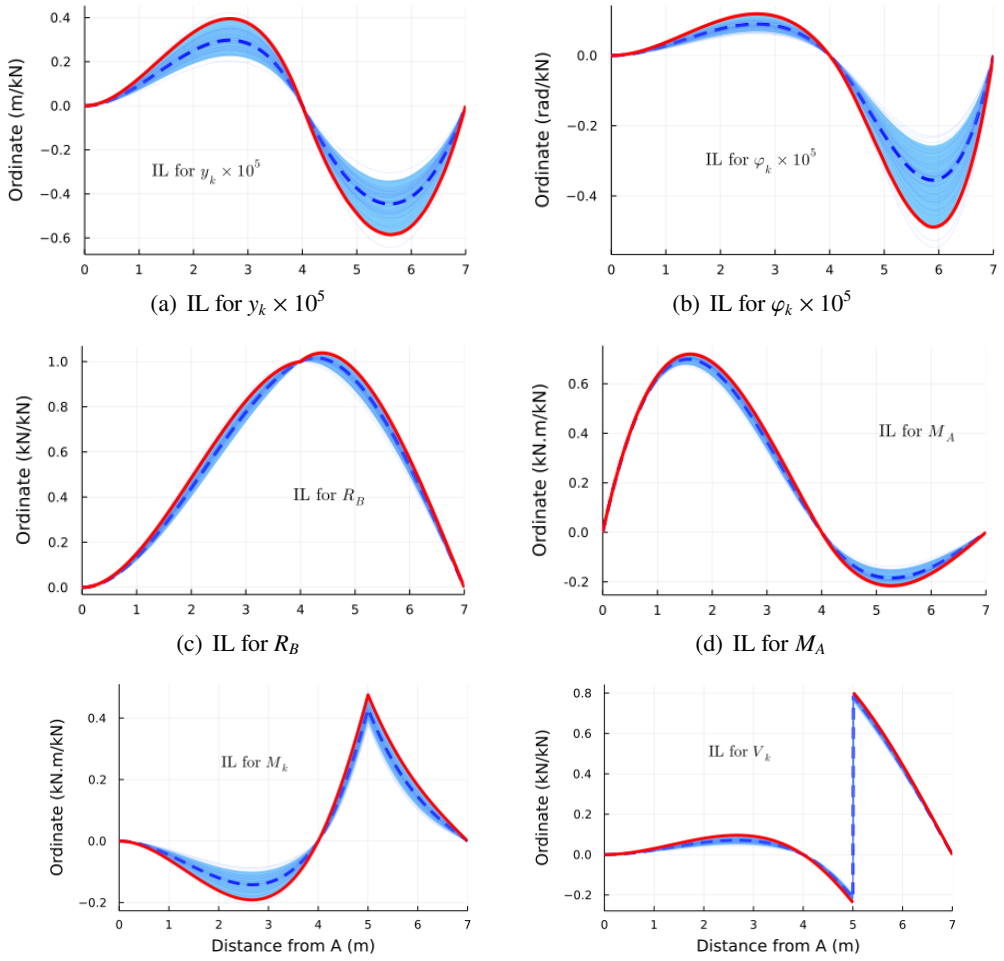

(a) IL for $y_k \times 10^5$ (b) IL for $\varphi_k \times 10^5$

(c) IL for R_B (d) IL for M_A

(e) IL for M_k (f) IL for V_k

Figure 6. Influences for responses (the samples of influence lines are shown in thin curves, mean curves are shown in blue dash, and red solid curves correspond to the worst-case with 98% confidence intervals)

To investigate the effect from the uncertainties in structure's properties to these IFs, the uncertainty propagation theory is then applied with help from the software package MonteCarloMeasurements.jl. Fig. 6 shows samples of influence lines as well as their confidence interval for each question from (a) to (g). The mean influence line is shown in bold blue dashed curve. The shaded band in light blue color shows the $(0.025, 0.0975)$ quantiles of the IFs (also called as the 98% confidence interval). The uncertainties from structural properties reflect most of the uncertainties of the translational/rotational displacement responses. Their shaded bands are larger compared with the shaded bands for reactions or for internal forces. The curve in red is the worst-case one with 98% confidence. The ratio between the absolute maximum value of the red curve and the corresponding blue dashed curve is about 1.4 for the case when the quantity S is rotational displacement at cross-section k, while the same value is about 1.3 for the case when the quantity S is translational displacement at k. It shows that even with small uncertainties in the structural properties, say less than 5% of the mean values, the uncertainties of the displacements are quite large, up to 30% or 40% of the mean values. In this example, the vertical reaction R_B is not affected much by the variations in the structural properties. It is easily checked that the influence line for the axial force N_k is identically equal to zero regardless of

any uncertain values of considered structural properties.

The propagations of uncertainties in structural geometry and in structural material properties are further investigated separately by ideally assuming that the structure of the uncertainties is fixed and dominated by a factor α. For the uncertainties in structural geometry, the width and the height of beam cross-section are correlated with each other by following covariance matrix.

$$\mathbf{\Sigma}_{b_1h_1} = \begin{bmatrix} 0.09 & 0.075 \\ 0.075 & 0.25 \end{bmatrix}\alpha^2, \quad \mathbf{\Sigma}_{b_2h_2} = \begin{bmatrix} 0.09 & 0.06 \\ 0.06 & 0.16 \end{bmatrix}\alpha^2 \tag{61}$$

For the uncertainties in structural material properties, Youngs' moduli of the two beams are correlated with each other by following covariance matrix.

$$\mathbf{\Sigma}_{E_1E_2} = 10^{14} * \begin{bmatrix} 5.29 & 2.88 \\ 2.88 & 6.25 \end{bmatrix}\alpha^2 \tag{62}$$

where α is taken as 0%, 1%, 2%, ..., 10%. The mean values of the structural properties are still the same as previously, namely,

$$\overline{E}_1 = 2.3\text{E}7, \quad \overline{E}_2 = 2.5\text{E}7, \quad \overline{b}_1 = 0.3, \quad \overline{h}_1 = 0.5, \quad \overline{b}_2 = 0.3, \quad \overline{h}_2 = 0.4 \tag{63}$$

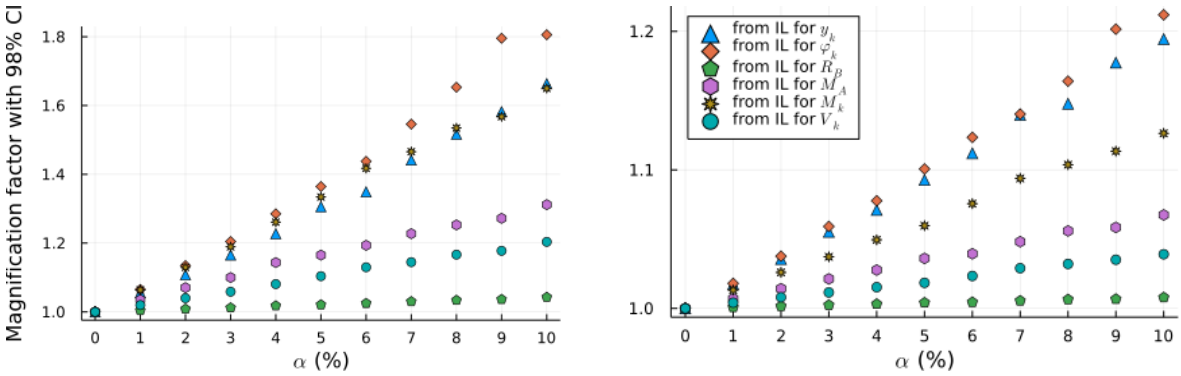

(a) (b)

Figure 7. Variations of magnification factor with 98% confidence intervals when there exist uncertainties: (a) in geometry of the structure; and (b) in materials of the structure

As mentioned earlier, the influence line for a quantity S varies depending on the uncertainty of the structural properties. Thus, for the safe design purposes, one might use the worst-case curve with 98% confidence intervals. By comparing this curve with the mean curve, in this example, we define a magnification factor with 98% confidence intervals as the ratio between the absolute values of the peaks in the worst-case curve and in the mean curve. This magnification factor is investigated as α changes its values. Fig. 7 shows the variations of this factor depending on the values of α. From Fig. 7, it is found that the six magnification factors with 98% confident interval are essentially linear functions of parameter α. It is also found that uncertainties in geometry of the structure affect much stronger to the magnification factor (to the influence lines) than uncertainties in materials of the structure do. When there are no uncertainties at all, the worst-case curves with 98% confidence intervals coincide with the mean curves and the corresponding magnification factors equal to unit. For the quantities under investigation, displacements at cross-section k are most affected by uncertainties in both geometry and materials of the structure, meanwhile the force reaction R_B is least affected by them. Fig. 7 also confirms the three quantities (y_k, φ_k, and M_k) for whom the influence lines are most affected by the parameter α showing the intensity of the given (structured) uncertainties.

5. Conclusions

The study systematically addressed a way to solve the problem of constructing influence lines for structural responses S using the combination of Muller-Breslau principle and the finite element approach. The structural responses might be a displacement at a cross-section, a reaction at a support, or one of internal forces at a particular section. For each situation, the corresponding equivalent nodal load vector is proposed. In situations where the quantity S is an internal force at a cross-section k, this study proposed new types of finite elements tailored for problems of drawing influence lines. Being different from other research, these elements already have in themselves the terms accounting for the local behavior. By that, these elements can be readily applicable to existing powerful finite element packages with only a few complexities introduced. Also, the model with these new elements can make ease the analysis of uncertainty propagation since for each set of uncertain properties of the structure, the finite element model is directly analyzed just once, without successively applying the unit load at many separate locations along the loading lane. The proposed method applies to both statically determinate and statically indeterminate structures. It can be applied to the case when S is a displacement, a reaction, an internal force, or even to the case when S is a linear combination of these structural responses. Application of the uncertainty propagation theory to obtain the uncertain influence lines for different structural responses shows that uncertainties in the ordinates of influence lines for displacements are larger compared with that of influence lines for reactions or internal forces. Numerical examples also show that, for unstructured uncertainties of the input, the uncertainties of the output responses increase linearly with respect to the input uncertainties. For design purposes, depending on the importance of the structure, the absolute maximum of 98% confidence interval of influence lines for structural responses might be used. A similar approach applied to smooth curve bar elements is on further study.

Acknowledgements

The author is thankful for the help from Julia community through https://stackoverflow.com and https://discours.julialang.org for effective use of MonteCarloMeasurement.jl, and Plots.jl. Symbolic formulas are obtained using SymPy.jl package.

References

[1] ÅKesson, B. Å., Bjarnehed, H. L., Anderson, H. O., Josefson, B. L. (1995). Routine FE determination of stress intensity factors using a Muller-Breslau influence function technique. *Fatigue & Fracture of Engineering Materials & Structures*, 18(10):1115–1132.

[2] Belegundu, A. D. (1988). The adjoint method for determining influence lines. *Computers & Structures*, 29(2):345–350.

[3] Cifuentes, A., Paz, M. (1991). A note on the determination of influence lines and surfaces using finite elements. *Finite Elements in Analysis and Design*, 7(4):299–305.

[4] Shen, W. (1992). The generalized Müller-Breslau principle for higher-order elements. *Computers & Structures*, 44(1-2):207–212.

[5] Memari, A. M., West, H. H. (1991). Computation of bridge design forces from influence surfaces. *Computers & Structures*, 38(5-6):547–556.

[6] Orakdogen, E., Girgin, K. (2005). Direct determination of influence lines and surfaces by FEM. *Structural Engineering and Mechanics*, 20(3):279–292.

[7] Yang, D., Chen, G., Du, Z. (2015). Direct kinematic method for exactly constructing influence lines of forces of statically indeterminate structures. *Structural Engineering and Mechanics*, 54(4):793–807.

[8] Welleman, H., van Eldik, C. H. (2016). *Work, energy methods and influence lines: Capita selecta in engineering mechanics*. Bouwen met staal.

[9] Jepsen, M. S., Damkilde, L. (2018). A direct and fully general implementation of influence lines/surfaces in finite element software. *Advances in Engineering Software*, 120:55–61.

[10] Hartmann, F., Jahn, P. (2021). *Statics and Influence Functions*. Springer International Publishing.
[11] Betti, E. (1872). Teoria della elasticita. *Il Nuovo Cimento*, 7-8(1):5–21.
[12] Tarnai, T., Lengyel, A. (2007). Reciprocal Theorems: An Old Subject Revisited. *International Journal of Mechanical Engineering Education*, 35(2):138–147.
[13] Maxwell, J. C. (1864). On the calculation of the equilibrium and stiffness of frames. *The London, Edinburgh, and Dublin Philosophical Magazine and Journal of Science*, 27(182):294–299.
[14] Gvozdev, A. A. (1927). *A general method for calculation of complex statically indeterminate systems*. MIIT, Moscow. (in Russian).
[15] Lien, T. V., Thang, N. T., Binh, N. T. (2013). Nondeteministic analysis of frame structure using interval finite element. *Journal of Science and Technology in Civil Engineering (STCE) - HUCE*, 7(1):18–29. (in Vietnamese).
[16] Taylor, J. (1997). *Introduction to error analysis, the study of uncertainties in physical measurements*. University Science Books, Sausalito, California, USA.
[17] Goodman, L. A. (1960). On the Exact Variance of Products. *Journal of the American Statistical Association*, 55(292):708–713.
[18] Carlson, F. B. (2020). MonteCarloMeasurements. jl: Nonlinear propagation of arbitrary multivariate distributions by means of method overloading. *arXiv preprint arXiv:2001.07625*.